Astron. Astrophys. 355, L1–L4 (2000)

ASTRONOMY AND ASTROPHYSICS

LETTER

Letter to the Editor

On the deuterium abundance at $z_{\rm a} = 3.514$ towards APM 08279+5255⋆

S.A. Levshakov[1,⋆⋆], **I.I. Agafonova**[1,⋆⋆], **and W.H. Kegel**[2]

[1] European Southern Observatory, 85748 Garching bei München, Germany
[2] Institut für Theoretische Physik der Universität Frankfurt am Main, 60054 Frankfurt/Main 11, Germany

Received 15 November 1999 / Accepted 28 January 2000

Abstract. A very low primordial deuterium abundance of $\rm D/H \simeq 1.5 \times 10^{-5}$ has recently been proposed by Molaro et al. in the Lyman limit system with $\log N_{\rm H\,\mathit{i}} \simeq 18.1$ cm^{-2} at $z_{\rm a} = 3.514$ towards the quasar APM 08279+5255. The D/H value was estimated through the standard Voigt fitting procedure utilizing a simple one-component model of the absorbing region. We have investigated this system using our new Monte Carlo inversion procedure which allows us to recover self-consistently both the physical parameters of the gas cloud and the projected velocity and density distributions along the line of sight. The absorption lines of H I, C II, C IV, Si III, and Si IV were analyzed simultaneously. The result obtained shows a considerably lower neutral hydrogen column density $\log N_{\rm H\,\mathit{i}} \simeq 15.7$ cm^{-2}. Hence, the measurement of the deuterium abundance in this system is rather uncertain. We find that the asymmetric blue wing of the hydrogen Lyα absorption is readily explained by H I alone. Thus, up to now, deuterium was detected in only four QSO spectra (Q 1937-1009, Q 1009+2956, Q 0130-4021, and Q 1718+4807) and all of them are in concordance with $\rm D/H \simeq 4 \times 10^{-5}$.

Key words: line: formation – line: profiles – galaxies: quasars: absorption lines – galaxies: quasars: individual: APM 08279+5255

1. Introduction

Accurate measurements of the hydrogen isotopic ratio D/H at high redshifts may allow us to test experimentally the basis of the standard model of big bang nucleosynthesis (BBN) – its homogeneity. A homogeneous BBN implies a *uniform* distribution of the D abundance among the absorbing systems with low metallicity since 'no realistic astrophysical process other than the Big Bang could produce significant D' (Schramm 1998, p.6).

First high quality spectral data of QSOs suggested, however, a dispersion in $\rm D/H \equiv N_{D\,\mathit{i}}/N_{H\,\mathit{i}}$ (the ratio of the D I and H I column densities) of about one order of magnitude (for a summary, see Burles et al. 1999). This finding provoked a lively discussion in the literature on inhomogeneous models of BBN (Dolgov & Pagel 1999 and references cited therein). But later, it was shown that a single D/H value of about 4×10^{-5} is sufficient to describe all observations available up to now (Levshakov et al. 1998a, 1998b, 1999b; Burles et al. 1999).

A new result by Molaro et al. (1999, hereafter MBCV), if confirmed, could challenge again the uniformity of the D/H space distribution because a very low deuterium abundance of $\rm D/H \simeq 1.5 \times 10^{-5}$ was suggested in an extremely low metallicity system at $z_{\rm a} = 3.514$ towards APM 08279+5255. MBCV consider the derived D abundance as a lower limit because their analysis was based on a simplified one-component model of the absorbing cloud which failed to fit the red wing of the Lyα line. They note that the observed complex structure of C IV and Si IV implies the presence of more than one component. They further state that 'additional components are required to reproduce the extra absorption on the red wing of Lyα' which would decrease the H I column density for the major component leading to a higher deuterium abundance.

Following the MBCV suggestions, we have analyzed the absorption profiles of H I, C II, C IV, Si III, and Si IV by using our new Monte Carlo inversion (MCI) algorithm (Levshakov et al. 2000, hereafter LAK). In the present Letter we show that the actual neutral hydrogen column density may be a factor of $\simeq 250$ lower than the value of MBCV, a fact preventing any accurate measurements of the deuterium abundance in the $z_{\rm a} = 3.514$ system.

The analysis by MBCV was performed in the framework of the one-component microturbulent model, whereas our approach is based on a more elaborated mesoturbulent model which describes the process of line formation in the absorbing clouds more adequately and in general implies a complex velocity field (Levshakov & Kegel 1997, LAK). In both cases

Send offprint requests to: S.A. Levshakov

⋆ Based on data obtained at the W. M. Keck Observatory, which is jointly operated by the California Institute of Technology, the University of California and the National Aeronautics and Space Administration.

⋆⋆ On leave from the Ioffe Physico-Technical Institute, Russian Academy of Sciences, 194021 St. Petersburg

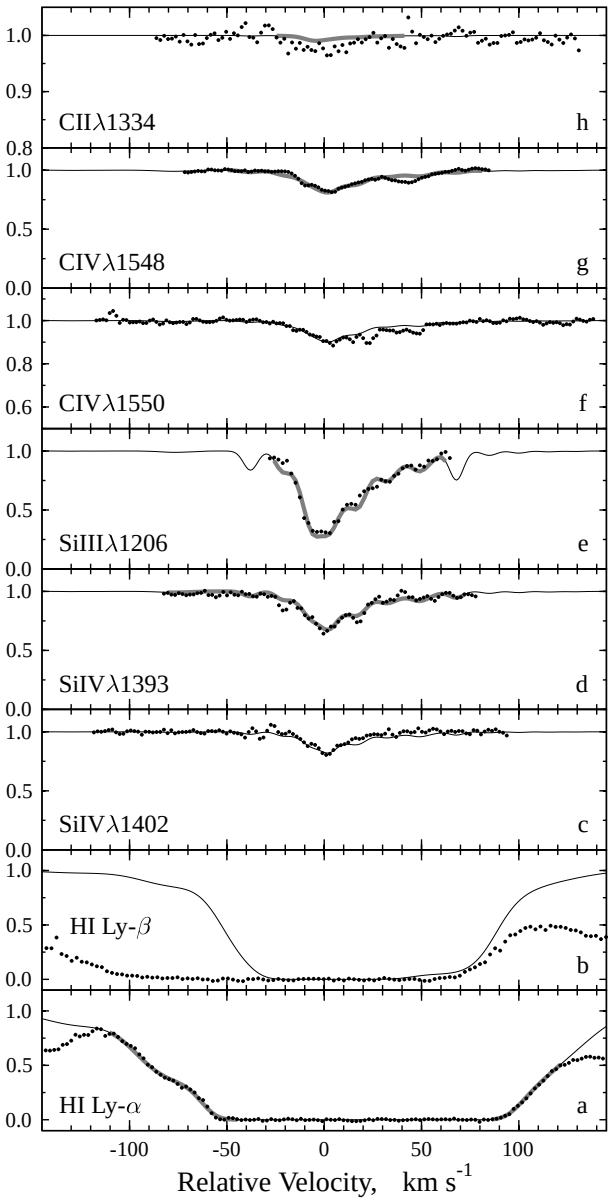

Fig. 1. Observed and synthetic line profiles of the absorption system at $z_{\rm a} = 3.514$ (model a, Table 1). Note different intensity scales in panels **h** and **f**. For details, see text

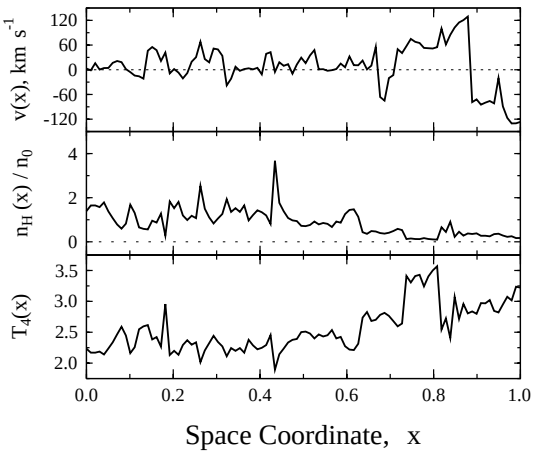

Fig. 2. MCI reconstruction of the radial velocity, density, and kinetic temperature distributions (model a, Table 1). T is given in units of 10^4 K

the same spectra of APM 08279+5255 obtained with the Keck-I telescope and the HIRES spectrograph by Ellison et al. (1999) are utilized.

2. Model assumptions and results

Our model supposes a continuous absorbing gas slab of a thickness L (presumably the outer region of a foreground galaxy). The absorber is assumed to exhibit a mixture of bulk motions such as infall and outflows, tidal flows etc. Then the gas motion along a given line of sight may be described by a fluctuating (random) velocity field in which the velocities in neighboring volume elements are correlated with each other (while in the standard microturbulent approximation completely uncorrelated velocities are assumed). The gas is tenuous and optically thin in the Lyman continuum. We are considering a compressible gas, i.e. the total number density of hydrogen $n_{\rm H}$ is also a random function of the space coordinate, x. Following Donahue & Shull (1991) and assuming that the ionizing radiation field is constant, the ionization of different elements can be described by one parameter only – the ionization parameter $U \propto 1/n_{\rm H}$. Furthermore, for gas in thermal equilibrium, Donahue & Shull give an explicit relation between U and the kinetic temperature T. The background ionizing spectrum in our model is taken from Mathews & Ferland (1987).

To estimate physical parameters and appropriate distributions of the velocity $v(x)$ and the normalized density $y(x) = n_{\rm H}(x)/n_0$, n_0 being the mean hydrogen density, we used the MCI procedure developed on the basis of the reverse Monte Carlo technique (Levshakov et al. 1999a). In our computations, the continuous random functions $v(x)$ and $y(x)$ are represented by their sampled values at equally spaced intervals Δx, i.e. by the vectors $\{v_1, ..., v_k\}$ and $\{y_1, ..., y_k\}$ with k large enough to describe the narrowest components of complex spectral lines. For the ionization parameter as a function of x, we have $U(x) = \hat{U}_0/y(x)$, with $\hat{U}_0$ being the reduced mean ionization parameter defined below. We fix $z_{\rm a} = 3.51374$ (the value adopted by MBCV) as a more or less arbitrary reference velocity at which $v_j = 0$.

Our aim is to fit the model spectra simultaneously to the observed hydrogen, carbon and silicon profiles. In this case the model requires the definition of a simulation box for the six parameters (see LAK, for details): the carbon and silicon abundances, $Z_{\rm C}$ and $Z_{\rm Si}$, respectively, the rms velocity $\sigma_{\rm v}$ and density dispersion $\sigma_{\rm y}$, the reduced total hydrogen column density $\hat{N}_{\rm H}\left[= N_{\rm H}/(1+\sigma_{\rm y}^2)^{1/2}\right]$, and the reduced mean ionization parameter $\hat{U}_0\left[= U_0/(1+\sigma_{\rm y}^2)^{1/2}\right]$. For the model parameters the following boundaries were adopted: $Z_{\rm C}$ ranges from 10^{-6} to 4×10^{-4}, $Z_{\rm Si}$ from 10^{-6} to 3×10^{-5}, $\sigma_{\rm v}$ from 25 to 80 km s^{-1}, $\sigma_{\rm y}$ from 0.5 to 2.2, $\hat{N}_{\rm H}$ from 5×10^{17} to 8×10^{19} cm^{-2}, and $\hat{U}_0$ ranges from 5×10^{-4} to 5×10^{-2}.

Having specified the parameter space, we minimize the χ^2 value. The objective function includes the following portions of the absorption profiles (labeled by grey lines in Fig. 1) which, after preliminary analysis, were chosen as most appropriate to the MCI fitting: for H I Lyα Δv ranges from -110 to -47 km s^{-1} (the blue wing) and from 84 to 119 km s^{-1} (the red wing, see Fig. 1a), for C II from -26 to 33 km s^{-1} (Fig. 1h), for C IVλ1548 from -51 to 79 km s^{-1} (Fig. 1g), for Si III from -28 to 60 km s^{-1} (Fig. 1e), and for Si IVλ1393 Δv ranges from -82 to 70 km s^{-1} (Fig. 1d). The necessity to choose these portions instead of all available profiles was caused by a few discrepancies in the data. Thus two small spikes in C IVλ1550 at $\Delta v = 15$ and 23 km s^{-1} are not seen in its stronger blue counterpart C IVλ1548, two minima in Si IVλ1393 at $\Delta v = -21$ and 17 km s^{-1} are invisible in the profile of the red component Si IVλ1402. Under these circumstances only the stronger blue components of the C IV and Si IV doublets were chosen for the analysis. But in Fig. 1 (panels **f** and **c**) the observed C IVλ1550 and, respectively, Si IVλ1402 are shown together with the model spectra computed with the parameters derived from Lyα, C IIλ1334, C IVλ1548, Si IIIλ1206, and Si IVλ1393 fitting to illustrate the consistency. For the same reason the Lyβ model spectrum is shown in Fig. 1b at the expected position. The additional absorption on the blueward and the redward sides of Lyβ in the observed spectrum may be caused by Lyα and/or Lyβ forest lines at different redshifts. In Fig. 1, all model spectra are drawn by continuous thin lines, whereas filled circles represent observations (normalized fluxes).

The MCI is a stochastic optimization procedure and one does not know in advance if the global minimum of the objective function is reached in a single run. Therefore we executed several runs for the given data set starting every calculation from a random point in the simulation box and from completely random configurations of the velocity and density fields. The results for five runs are listed in Table 1. The first solution (model a in Table 1) was used to calculate the synthetic spectra shown in Fig. 1, and the corresponding distributions of $v(x)$, $y(x)$, and $T(x)$ which are presented in Fig. 2. The derived configurations of these random fields are not unique: any simultaneously made permutation of the components in the $\{v_1, ..., v_k\}$ and $\{y_1, ..., y_k\}$ vectors is acceptable since the permutated patterns produce the same density-weighted radial velocity distribution which can actually be constrained from the analysis of profiles of different ions. Details of the formal procedure and to which extent model parameters can be recovered, are discussed in LAK.

With $N_{\rm H} = 5.9 \times 10^{18}$ cm^{-2}, $N_{{\rm H}\,i} = 5.3 \times 10^{15}$ cm^{-2}, $U_0 = 1.6 \times 10^{-2}$, $\sigma_{\rm v} = 51$ km s^{-1}, $\sigma_{\rm y} = 1.1$, [C/H] = – 1.8, and [Si/H] = – 0.7 the median estimated parameters are close to those of model c. The results were obtained with $k = 100$ and the correlation coefficients $f_{\rm v} = f_{\rm y} = 0.95$.

The MCI allowed us to fit precisely not only the blue wing of the saturated Lyα line but the red one as well. In addition we have reached a reasonable concordance between hydrogen and metal absorption lines. Although our model spectra of metal lines are consistent with the observed profiles within the 3-σ uncertainty range, we found difficulties with the C II line fitting. The C II model spectrum lies systematically over the observed intensities (Fig. 1h). We note that the measurement of the C II line depends sensitively on the exact definition of the continuum because the line is very weak.

Table 1. Cloud parameters derived from the Lyα and metal profiles by the MCI procedure (the total hydrogen column density $N_{18}^{\rm H}$ in units of 10^{18} cm^{-2}, the neutral hydrogen column density $N_{15}^{{\rm H}\,i}$ in units of 10^{15} cm^{-2}, the mean ionization parameter U_{-2}^0 in units of 10^{-2}, the rms velocity $\sigma_{\rm v}$ in km s^{-1}, the reduced $\frac{1}{\nu}\chi^2_{{\rm H}\,i}$ per degree of freedom, $\nu = 42$, for the Lyα blue and red wings)

	$N_{18}^{\rm H}$	$N_{15}^{{\rm H}\,i}$	U_{-2}^0	$\sigma_{\rm v}$	$\sigma_{\rm y}$	[C/H]*	[Si/H]*	$\frac{1}{\nu}\chi^2_{{\rm H}\,i}$
a	4.4	4.6	1.25	51	1.1	-1.7	-0.6	1.17
b	5.0	5.3	1.10	50	0.8	-1.8	-0.7	1.15
c	5.9	5.2	1.60	48	1.1	-1.8	-0.7	1.16
d	8.7	7.2	2.54	70	1.6	-1.9	-0.8	1.16
e	11.3	8.1	1.83	52	0.9	-2.1	-0.9	1.03

* based on solar abundances from Grevesse (1984);
[X/H] = $\log(N_{\rm X}/N_{\rm H}) - \log(N_{\rm X}/N_{\rm H})_\odot$

Nevertheless, let us assume for a moment that MBCV's measurement of C II is correct, and let us compare in some more detail the results obtained by MBCV with ours. Using the Doppler parameters $b_{{\rm C}\,ii} = 17.8 \pm 1.8$ km s^{-1} and $b_{{\rm H}\,i} = 21.0 \pm 0.6$ km s^{-1} measured by MBCV, it is easy to estimate the turbulent velocity $\sigma_{\rm v,mic} \equiv b_{\rm turb}/\sqrt{2} = 12.4 \pm 6.1$ km s^{-1} and the kinetic temperature $T_{\rm mic} = 8280 \pm 4590$ K. On the other side, the MCI kinetic temperature distribution (Fig. 2) does not reveal values lower than 2×10^4 K. Furthermore, the mean $T_{\rm mic} = 8280$ K seems to be too low for the photoionization heating. The mean kinetic temperature from the mesoturbulent solution $T_{\rm meso} = 25500$ K is, probably, more realistic. The four times higher mesoturbulent value of the rms velocity can be expected from observations of this quasar. Indeed, large broadening may be caused by the lensing effects since this QSO exhibits two components of similar intensity separated by $\sim 0''.4$ (Irvin et al. 1998).

3. Conclusions

We have shown that the $z_a = 3.514$ system can be described by a set of parameters strongly different from that obtained by MBCV. In particular, the Lyα profile can be modeled with a considerably lower value of $N_{{\rm H}\,i}$ if one accounts for a more complex velocity field structure. This implies that the identification of the D I line in this system cannot be confirmed or ruled out without additional observations of the higher order Lyman series lines in order to constrain the total neutral hydrogen column density and the velocity field configuration.

For this particular case, the presence of the extra-absorption at the expected deuterium position $\Delta v = -82$ km s^{-1} becomes evident from the upper panel of Fig. 3 where dotted and solid line histograms show, respectively, the density-weighted radial velocity distributions $p(v)$ for the total and neutral hydrogen (model a, Table 1), whereas the dashed curve illustrates $p(v)$ as

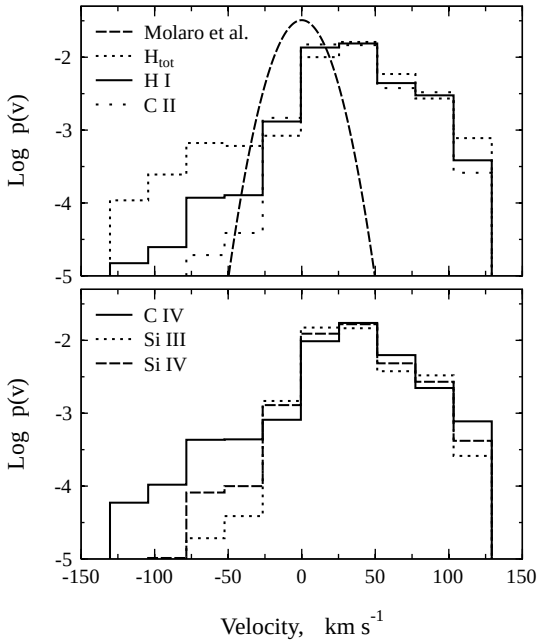

Fig. 3. Density-weighted radial velocity distribution functions, $p(v)$, for the total and neutral hydrogen, C II, C IV, Si III, and Si IV as restored by the MCI procedure (model a, Table 1). For comparison, in the upper panel the short dashed curve shows $p(v)$ for the homogeneous microturbulent model adopted by MBCV

adopted by MBCV (a Gaussian with $\sigma_{\rm v,mic} = 12.4$ km s^{-1}). The radial velocity distribution of H I is asymmetric with a long tail towards the blue side which may just mimic the deuterium absorption. The main maximum of $p_{{\rm H}\,i}(v)$ is shifted to $\Delta v \simeq 30$ km s^{-1} with respect to MBCV' frame of reference. The distribution $p_{{\rm H}\,i}(v)$ exhibits also an extended red wing ranging up to $\Delta v \simeq 100$ km s^{-1}. This asymmetry is also clearly pronounced in the Si III profile (Fig. 1e). Other models, listed in Table 1, show practically the same $p(v)$-distributions.

The restored density and velocity fields reveal a complex structure which is manifested in non-Gaussian distributions as shown in Fig. 3 for the total hydrogen density as well as for the individual ions. It appears that C IV is a good tracer for the distribution of the total hydrogen density in this particular case.

We also do not confirm the extremely low metallicity of $[{\rm C/H}] \simeq -4.0$ and $[{\rm Si/H}] \simeq -3.5$ reported by MBCV. Our analysis yields considerably higher values of $[{\rm C/H}] \simeq -1.8$ and $[{\rm Si/H}] \simeq -0.7$. A metallicity as high as [C/H] $\simeq -1$ and a silicon overabundance [Si/C] $= 0.5-1$ dex has been measured et al. in the metal systems at $z_{\rm a} \sim 4$ towards Q 0000–2619 (Savaglio 1997). A similar silicon overabundance has also been observed in halo (population II) stars. The standard interpretation of these observations is that the metal-poor gas was enriched by Type II supernova nucleosynthesis products (e.g. Henry & Worthey 1999). Thus, our measurements are in agreement with these results.

Hence, it may be concluded that up to now deuterium lines have been identified in only four QSO spectra. Our previous D/H measurements in Q 1937–1009, Q 1009+2956, and probably in Q 1718+4807, and the last one by Kirkman et al. (1999) in Q0130–4021 are consistent with a single value of ${\rm D/H} \simeq 4 \times 10^{-5}$.

Acknowledgements. The authors are grateful to Ellison et al. for making their data available. We thank Sandro D'Odorico for valuable comments and Miguel Albrecht for kind advice in using the ESO computer cluster. We also thank David Tytler and another anonymous referee for their helpfull reports. SAL and IIA gratefully acknowledge the hospitality of the European Southern Observatory (Garching), where this work was performed.

References

Burles, S., Kirkman, D., Tytler, D. 1999, ApJ, 519, 18
Dolgov, A. D., Pagel, B. E. J. 1999, New Astron., 4, 223
Donahue, M., Shull, J. M. 1991, ApJ, 383, 511
Ellison, S. L. et al. 1999, PASP, 111, 946
Grevesse, N. 1984, Phys. Scripta, T8, 49
Henry, R. B. C., Worthey, G. 1999, PASP, 111, 919
Irwin, M. J. et al. 1998, ApJ, 505, 529
Kirkman, D. et al. 1999, AAS, 194, 3001
Levshakov, S. A., Kegel, W. H. 1997, MNRAS, 288, 787
Levshakov, S. A., Kegel, W. H., Takahara, F. 1998a, ApJ, 499, L1
Levshakov, S. A., Kegel, W. H., Takahara, F. 1998b, A&A, 336, L29
Levshakov, S. A., Kegel, W. H., Takahara, F. 1999a, MNRAS, 302, 707
Levshakov, S. A., Tytler D., Burles S. 1999b, in Proceed. of the Gamov Memorial International Conference, St. Petersburg, August 23-28, 1999), in press
Levshakov, S. A., Agafonova, I. I., Kegel, W. H. 2000, A&A, submit. [LAK]
Mathews, W. D., Ferland, G. 1987, ApJ, 323, 456
Molaro, P. et al. 1999, A&A, 349, L13 [MBCV]
Savaglio, S. et al. 1997, A&A, 318, 347
Schramm, D. N. 1998, in *Primordial Nuclei and Their Galactic Evolution*, eds. N. Prantzos, M. Tosi, & R. von Steiger (Kluwer Academic Publ.: Dordrecht, The Netherlands), 3